Supplementary Information

Chemical derivatization of citrullinated peptides using methylglyoxal and sodium 3-mercaptopropanesulfonate (MG/MPS)

Yunxia Wang[a,1], Juanjuan Zhao[b,1], Shan Zhang[a], Ying Wang[a], Zhibo Jin[a], Xingtai Qiu[c], Zichao Tang[c], Nan Deng[d*], Yangyang Bian[a*]

a Key Laboratory of Resource Biology and Modern Biotechnology in Western China, College of Life Science, Northwest University, Xi'an, Shaanxi Province 710069, P.R. China.

b Department of Pharmacy, General Hospital of Ningxia Medical University, No.804 Shengli South Street, Yinchuan, Ningxia, 750004, PR China.

c Xiamen Jinnuohua Biotechnology Co., Ltd., Xiamen, Fujian, 361000, P.R. China.

d Instrumental Analysis Center, Xi'an Jiaotong University, Xi'an, Shaanxi Province 710049, P.R. China.

* Corresponding authors.

E-mail addresses: dengnan@xjtu.edu.cn, bianyy@nwu.edu.cn

[1] These authors contributed equally to this work.

Figures

Figure S1.

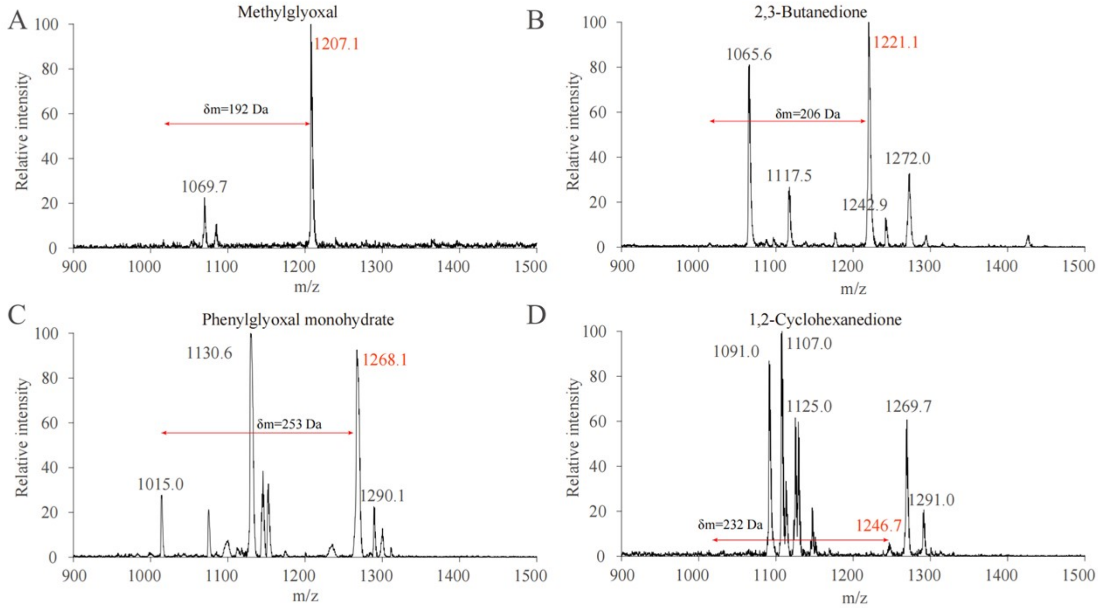

Figure S1. MALDI-TOF MS spectrum of the standard citrullinated peptide PL-Cit-AASPFR after derivatization with different dicarbonyl compounds and sodium 3-mercaptopropanesulfonate. (A) methylglyoxal, (B) 2,3-butanedione, (C) phenylglyoxal monohydrate, (D) 1,2-cyclohexanedione.

Figure S2.

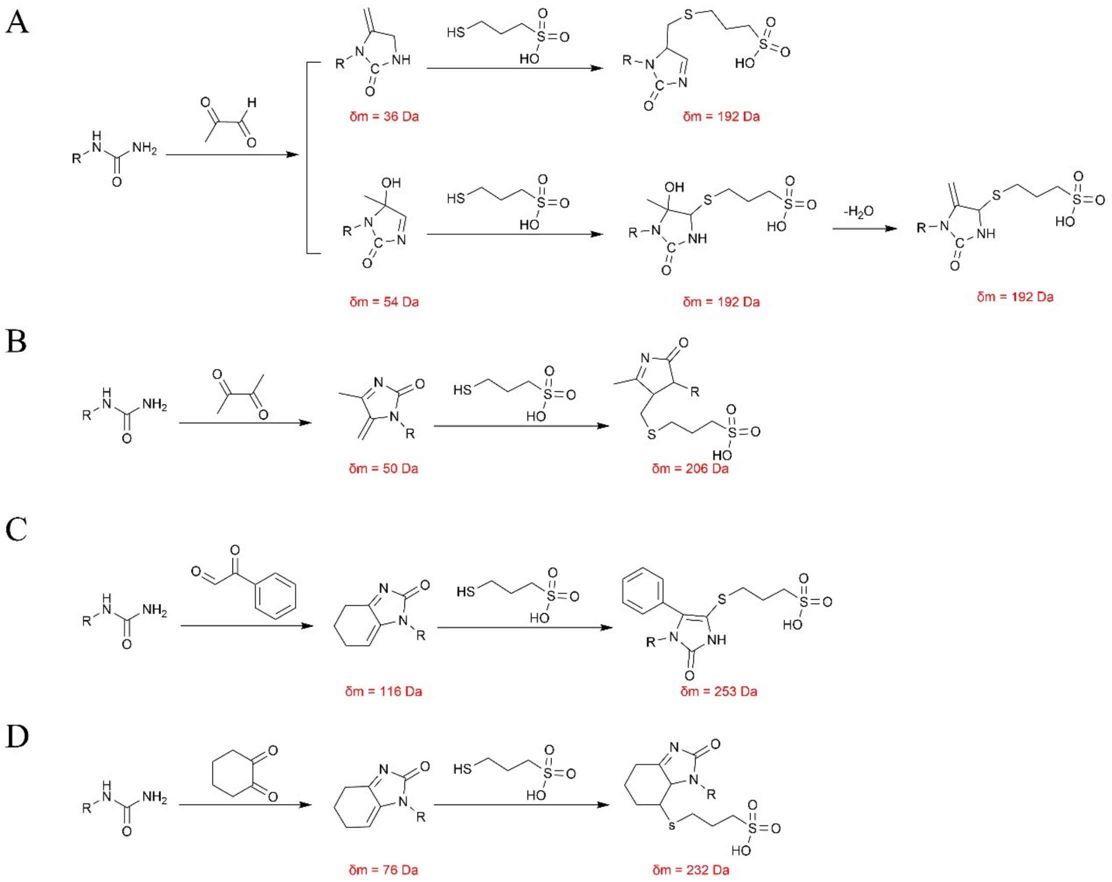

Figure S2. Reaction mechanism diagram of the standard peptide with different dicarbonyl compounds and sodium 3-mercaptopropanesulfonate. (A) methylglyoxal, (B) 2,3-butanedione, (C) phenylglyoxal monohydrate, (D) 1,2-cyclohexanedione.

Figure S3.

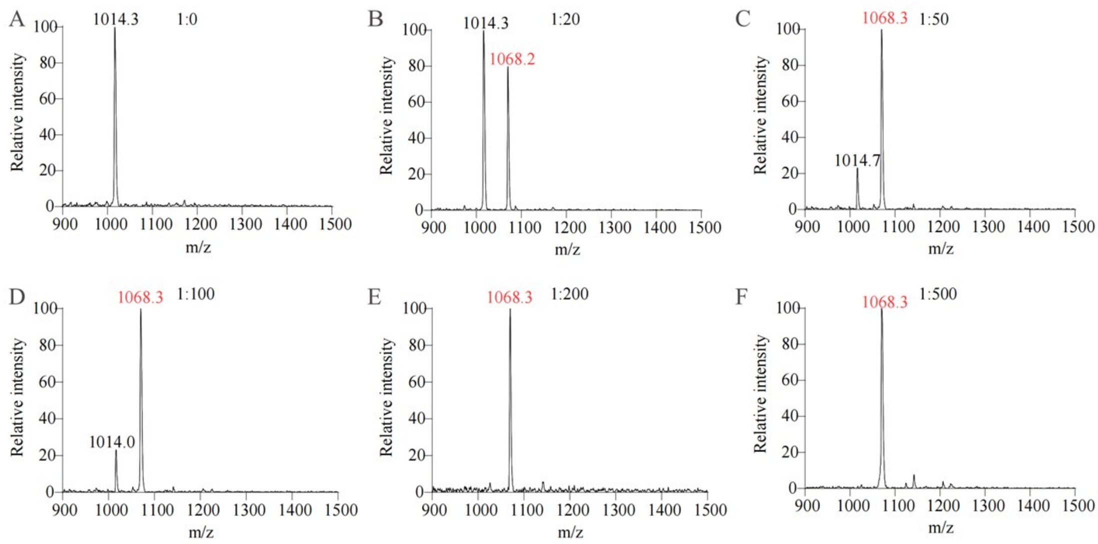

Figure S3. MALDI-TOF MS spectrum of the standard citrullinated peptide PL-Cit-AASPFR after derivatization with different ratios of methylglyoxal. (A) 1:0, (B) 1:20, (C) 1:50, (D) 1:100, (E) 1:200, (F) 1:500.

Figure S4.

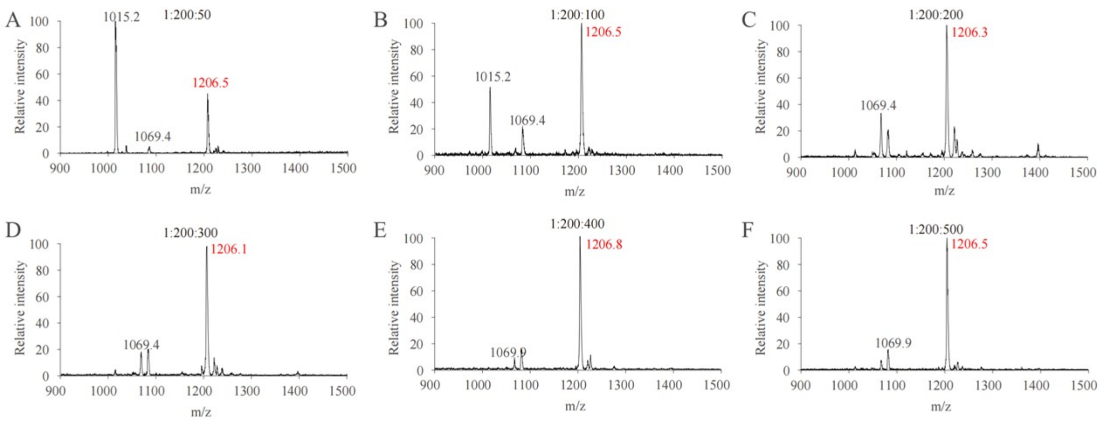

Figure S4. MALDI-TOF MS spectrum of the standard citrullinated peptide PL-Cit-AASPFR after derivatization with methylglyoxal and different ratios of sodium 3-mercaptopropanesulfonate. (A) 1:200:50, (B) 1:200:100, (C) 1:200:200, (D) 1:200:300, (E) 1:200:400, (F) 1:200:500.

Figure S5

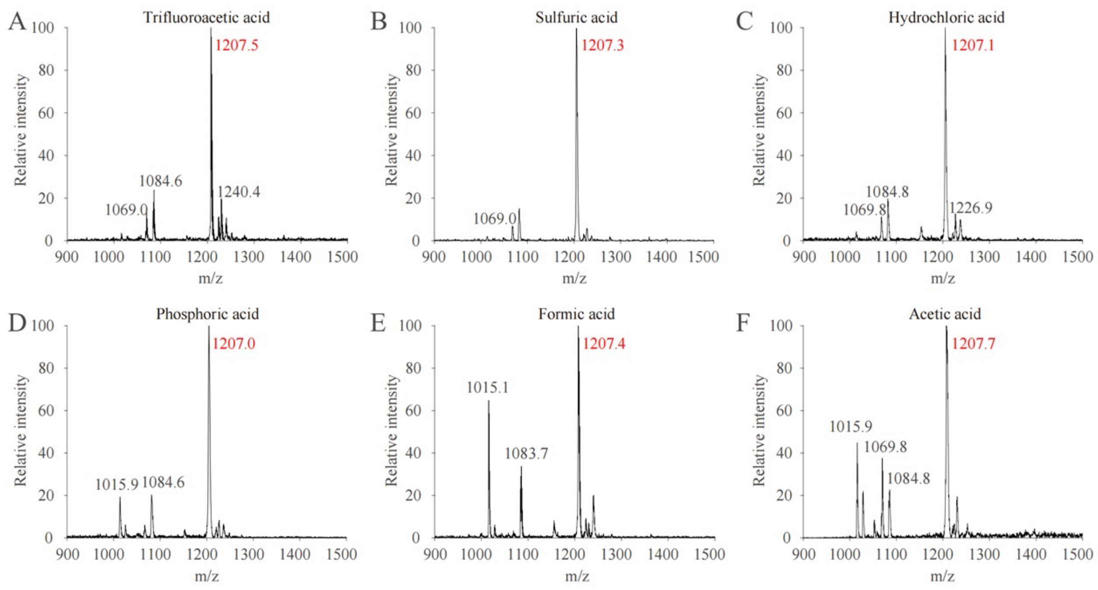

Figure S5. MALDI-TOF MS spectrum of the standard citrullinated peptide PL-Cit-AASPFR after derivatization with methylglyoxal, sodium 3-mercaptopropanesulfonate, and different types of acids. (A) 10% trifluoroacetic acid, (B) 10% sulfuric acid, (C) 10% hydrochloric acid, (D) 10% phosphoric acid, (E) 10% formic acid, (F) 10% acetic acid.

Figure S6.

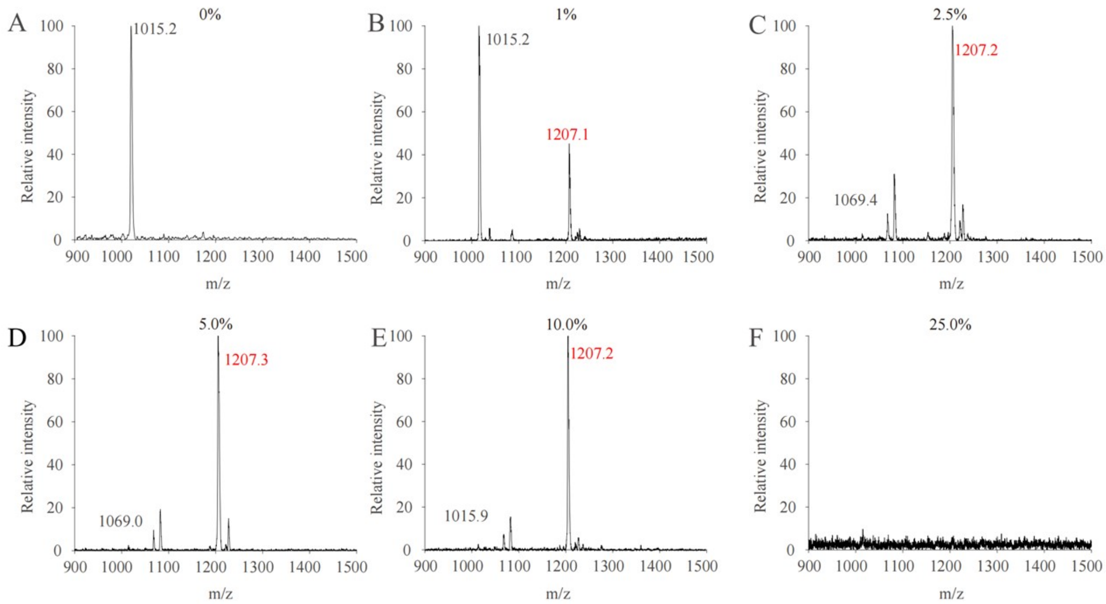

Figure S6. MALDI-TOF MS spectrum of the standard peptide PL-Cit-AASPFR after derivatization with methylglyoxal, sodium 3-mercaptopropanesulfonate, and different concentrations of sulfuric acid. (A) 0%, (B)1%, (C) 2.5%, (D) 5.0%, (E) 10.0%, (F) 25.0%.

Figure S7.

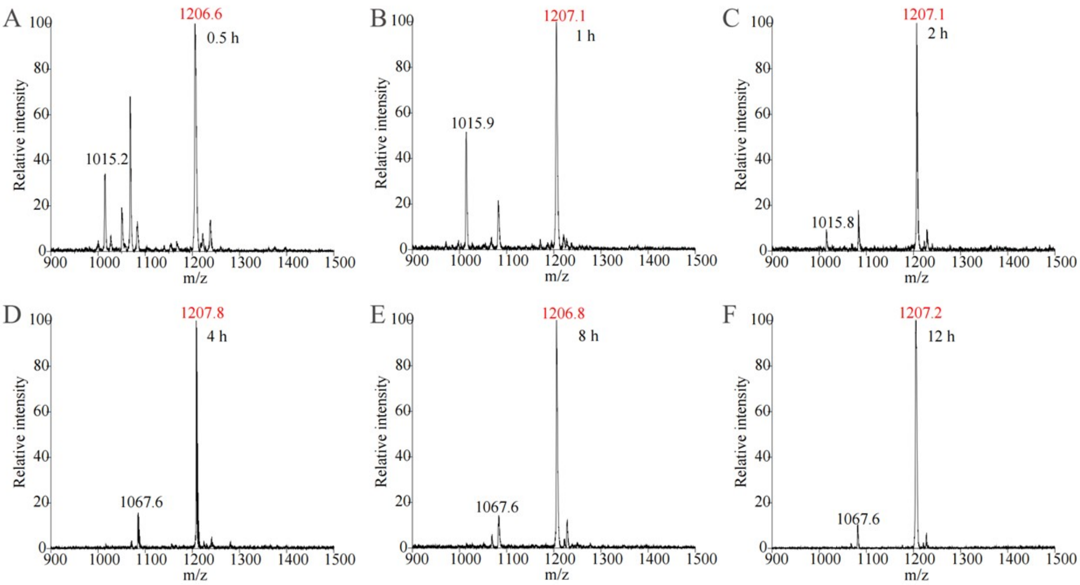

Figure S7. MALDI-TOF MS spectrum of the standard peptide PL-Cit-AASPFR after derivatization with methylglyoxal and sodium 3-mercaptopropanesulfonate at different reaction times. (A) 0.5 h, (B) 1 h, (C) 2 h, (D) 4 h, (E) 8 h, (F) 10 h.

Figure S8.

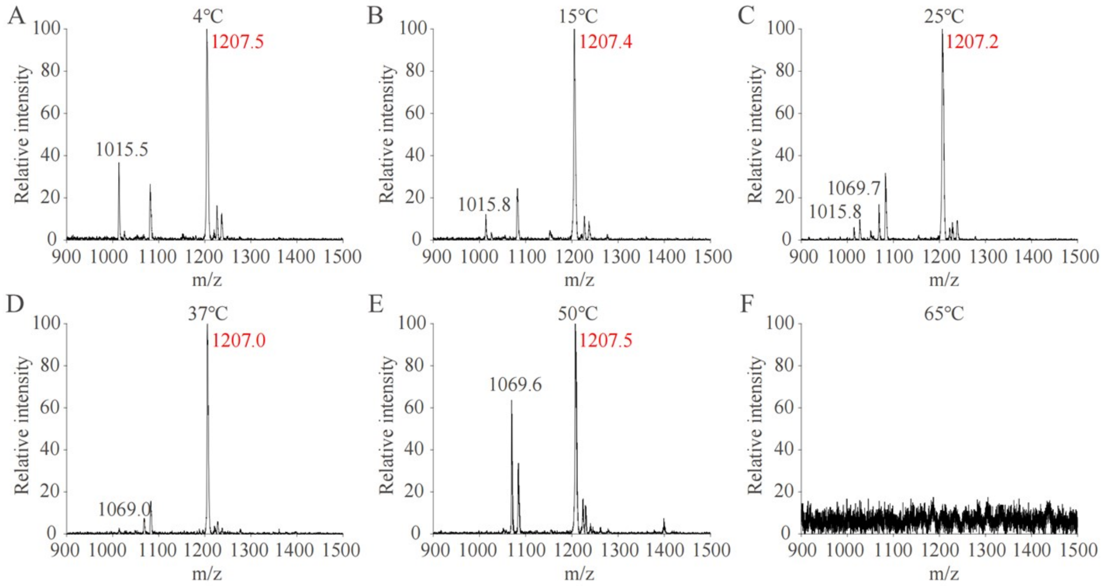

Figure S8. MALDI-TOF MS spectrum of the standard peptide PL-Cit-AASPFR after derivatization with methylglyoxal and sodium 3-mercaptopropanesulfonate at different reaction temperatures. (A) 4°C, (B) 15°C, (C) 25°C, (D) 37°C, (E) 50°C, (F) 65°C.

Figure S9.

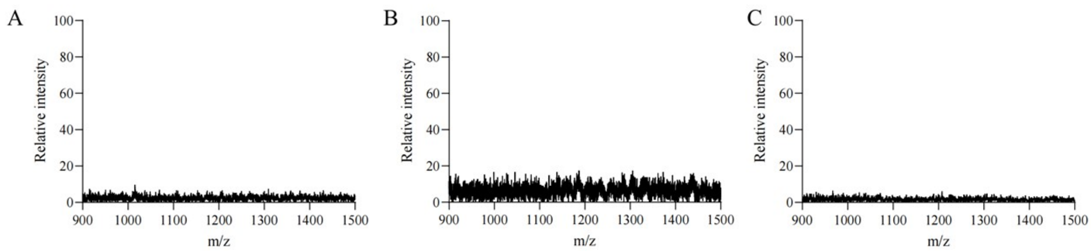

Figure S9. MALDI-TOF MS spectrum of three independent replicate experiments for the standard peptide PL-Cit-AASPFR after derivatization with methylglyoxal and sodium 3-mercaptopropanesulfonate at 65°C. (A, B, C) Results of three independent replicate experiments, respectively.

Figure S10.

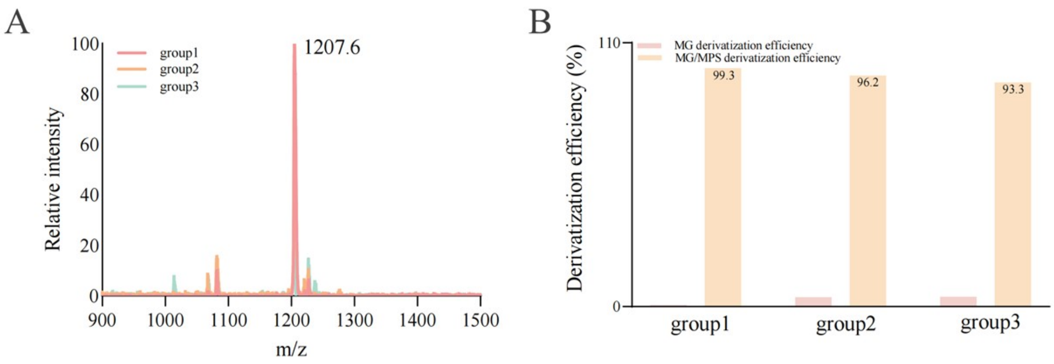

Figure S10. Validation of derivatization efficiency and reproducibility of the MG/MPS derivatization strategy using the citrullinated peptide PL-Cit-AASPFR. Derivatization was performed as described in the workflow section (see materials and methods for details). (A) Overlaid MALDI-TOF MS spectra of the derivatized citrullinated peptide from three parallel experiments. (B) Bar graph showing the derivatization efficiency of the MG/MPS strategy across three independent experiments.

Figure S11.

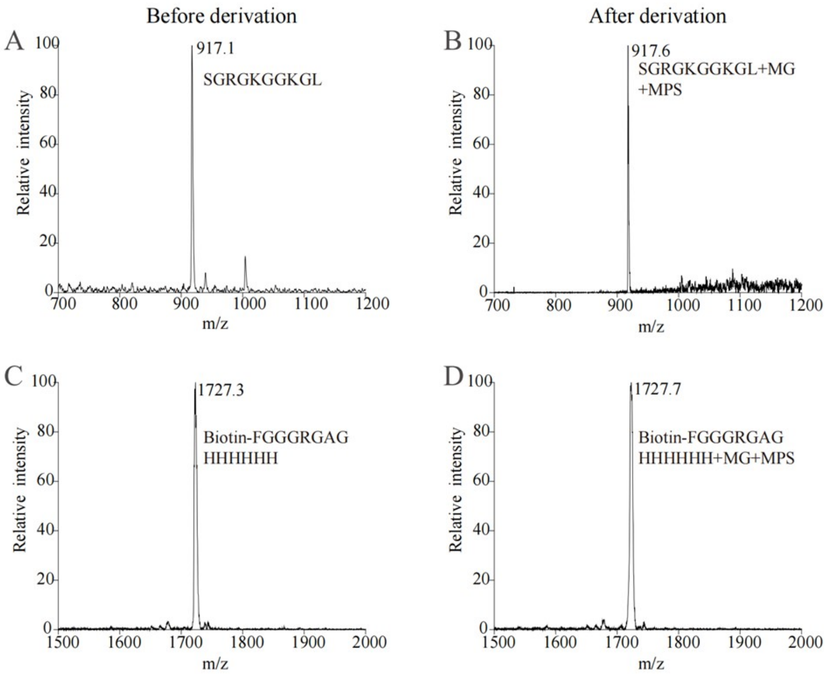

Figure S11. MALDI-TOF MS spectrum of two arginine-containing peptides SGRGKGGKGL and Biotin-FGGGRGAGHHHHHH before (A, C) and after (B, D) methylglyoxal and sodium 3-mercaptopropanesulfonate derivatization.

Figure S12.

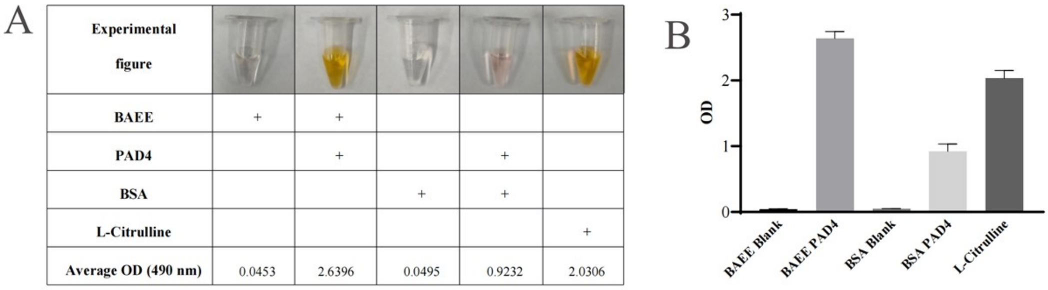

Figure S12. Qualitative and quantitative analysis of PAD4-catalyzed citrullination via COLDER assay. (A) Experimental grouping and tabulation of average optical density (OD) values at 490 nm, paired with visual colorimetric reaction results for each sample. BAEE was used as a small-molecule substrate for PAD4, BSA as the protein substrate, and L-citrulline as a positive control for the color-developing reagent. (B) Quantitative bar graph of OD values at 490 nm for all samples, confirming PAD4 enzymatic activity toward both BAEE and BSA.

Figure S13.

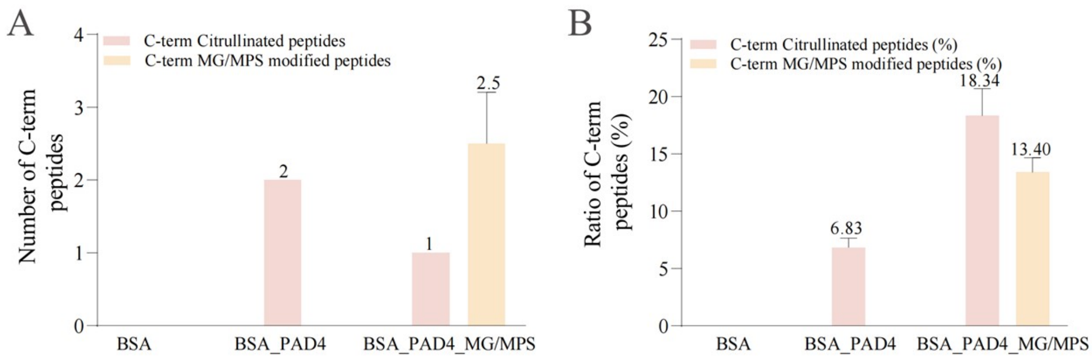

Figure S13. Analysis of C-terminal citrullinated and MG/MPS-modified peptides in three experimental groups. (A) Bar chart showing the number of C-terminal citrullinated peptides and C-terminal MG/MPS modified peptides across three experimental groups (BSA, BSA_PAD4, BSA_PAD4_MG/MPS). (B) Bar chart displaying the percentage ratio of C-terminal citrullinated peptides and C-terminal MG/MPS modified peptides relative to total identified peptides across three experimental groups (BSA, BSA_PAD4, BSA_PAD4_MG/MPS).

Figure S14.

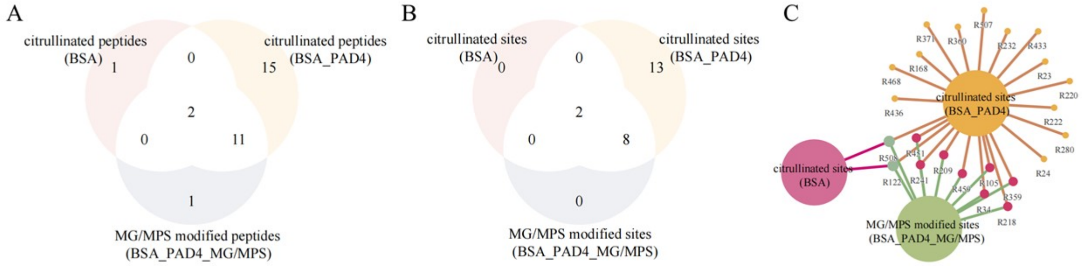

Figure S14. Overlap analysis of citrullinated peptides and modification sites in BSA samples. (A) Venn diagram showing the overlap of modified peptides identified across the three experimental groups. (B) Venn diagram illustrating the overlap of citrullination modification sites identified across the three experimental groups. (C) Network visualization of citrullinated modification sites identified in BSA samples across the three experimental groups.

Figure S15.

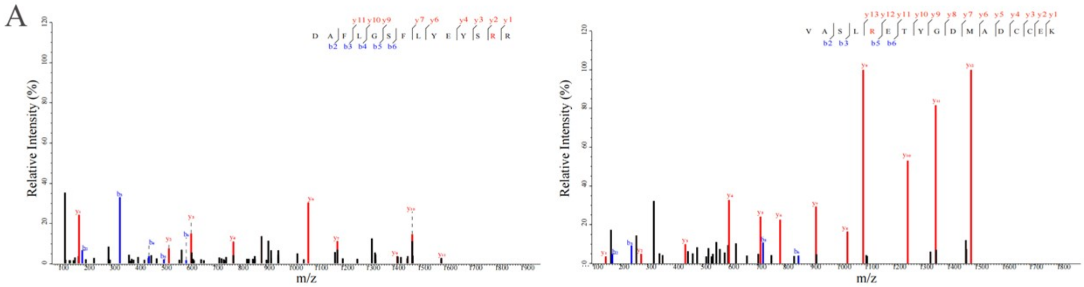

Figure S15. Representative MS/MS spectra of identified MG/MPS-modified citrullinated peptides.